DOI: 10.1002/cmdc.200800443

Homology Model Adjustment and Ligand Screening with a Pseudoreceptor of the Human Histamine H_4 Receptor

Yusuf Tanrikulu,[a] Ewgenij Proschak,[a] Tim Werner,[a] Tim Geppert,[a] Nickolay Todoroff,[a] Alexander Klenner,[a] Tim Kottke,[b] Kerstin Sander,[b] Erich Schneider,[c] Roland Seifert,[d] Holger Stark,[b] Timothy Clark,[e] and Gisbert Schneider*[a]

A computer-assisted method for the generation of pseudoreceptor models is presented together with two practical applications. From a three-dimensional alignment of known histamine H_4 receptor ligands, a pseudoreceptor model of the putative ligand binding site was constructed and used for virtual screening of a large collection of commercially available compounds. Two bioactive chemotypes were retrieved, demonstrating the general applicability of the approach. The pseudoreceptor model was also used to find the putative ligand binding pocket within the transmembrane receptor domain. For each frame of a molecular dynamics simulation of a homology-based H_4 receptor model, we automatically extracted potential ligand binding pockets and used their compatibility with the pseudoreceptor as a selection criterion. The best-matching pocket fits perfectly with existing mutation data and previously published hypotheses suggesting Glu182$^{5.46}$ as the preferred binding partner of a positively charged moiety of H_4 receptor ligands. This new pseudoreceptor approach has demonstrated its suitability for both structure-based prioritization of protein receptor models, and ligand-based virtual screening with the aim to perform scaffold hopping.

Introduction

Ligand- and receptor-based in silico methods are complementary concepts in pharmaceutical drug research and development.[1] Both provide methodologically distinct and worthwhile approaches to hit and lead identification. Whereas receptor-based methods rely on a three-dimensional (3D) model of the ligand-binding pocket, ligand-based techniques can be applied in the absence of a known or modeled receptor protein structure. The idea of pseudoreceptor modeling is to link both domains of virtual screening.[2] Herein, we present a new interpretation and implementation of the pseudoreceptor concept along with practical applications.

The absence of 3D receptor information poses a particular challenge in drug design projects targeting G protein coupled receptors (GPCRs). A limited number of membrane protein crystal structures permits restricted use of receptor-based programs.[3] As there are only limited advances in structure determination methods,[4] receptor information is usually gained through homology modeling[5] based on sequence similarity assessment and subsequent structural alignment of related protein family members.[6] Several 3D quantitative structure–activity relationship (QSAR) techniques were introduced representing hybrid systems,[7] which correlate ligand topologies or physicochemical properties with activities to direct toward putatively interesting (often activity rising) regions of ligand binding pockets.[8] Pseudoreceptor modeling is another 3D QSAR branch pioneered more than two decades ago.[9] Pseudoreceptor models are based on the construction of virtual binding pockets around one or more reference ligands by capturing their shape and/or important interaction points.

Herein, we present the development of an automated pseudoreceptor construction algorithm (PRPS, pseudoreceptor point similarity) and its applications. First, we describe the model construction algorithm. Secondly, we demonstrate how to transfer ligand information into a homology-based receptor model by PRPS. As an example we chose the identification of a putative histamine H_4 receptor (H_4R) antagonist binding pocket from a molecular dynamics (MD) simulation of a H_4R homology model. In the final part, a preliminary prospective screening for new H_4R ligands is presented, which illustrates

[a] *Y. Tanrikulu, Dr. E. Proschak, T. Werner, T. Geppert, N. Todoroff, A. Klenner, Prof. Dr. G. Schneider*
Chem- and Bioinformatics LiFF/ZAFES/CMP
Johann Wolfgang Goethe University
Siesmayerstr. 70, 60323 Frankfurt a.M. (Germany)
Fax: (+49) 69-798-24880
E-mail: g.schneider@chemie.uni-frankfurt.de

[b] *T. Kottke, K. Sander, Prof. Dr. H. Stark*
Institute of Pharmaceutical Chemistry LiFF/ZAFES/CMP
Johann Wolfgang Goethe University
Max-von-Laue Str. 9, 60438 Frankfurt a.M. (Germany)

[c] *Dr. E. Schneider*
Department of Pharmacology and Toxicology, University of Regensburg
Universitätsstr. 31, 93053 Regensburg (Germany)

[d] *Prof. Dr. R. Seifert*
Institute of Pharmacology, Medical School of Hannover
Carl-Neuberg-Str. 1, 30625 Hannover (Germany)

[e] *Prof. Dr. T. Clark*
Computer Chemistry Centre, University of Erlangen-Nürnberg
Naegelsbachstr. 25, 91052 Erlangen (Germany)

Supporting information for this article is available on the WWW under http://dx.doi.org/10.1002/cmdc.200800443.

the applicability of the PRPS descriptor for hit retrieval by virtual screening.

Results and Discussion

Pseudoreceptor construction method

The basis of pseudoreceptor construction is the knowledge of at least one active reference ligand. If a ligand ensemble is used, the molecular structures must be provided as a 3D alignment. The main idea of our automated pseudoreceptor construction package PRPS is to project pseudoatoms around ligand interaction sites (potential pharmacophore points, PPP). Pseudoatoms delineate putative receptor atom positions. They are positioned according to hydrogen bond constraints found in a crystal survey of the Protein Data Bank (PDB).[10] PRPS pseudoreceptor generation consists of four steps: 1) grid assembly, 2) deletion of invalid points, 3) identification of PPPs, and 4) pseudoatom projection. The procedural method is to pinpoint putative receptor atom positions by selecting valid grid points as pseudoatoms. The set of all pseudoatoms composes the final pseudoreceptor model:

1. First, a cubic grid is assembled around the reference ligands with a 5 Å margin in each direction and 0.5 Å grid spacing.
2. As each grid point may be selected as a putative receptor atom, invalid points (with distance less than the van der Waals (vdW) radius of the next ligand atom) are deleted, based on vdW potentials.[1]
3. Ligand atoms, which are capable of forming hydrogen bridges, are identified as anchor atoms according to the procedure introduced by Mills and Dean.[10]
4. Grid points with valid hydrogen bonding constraints are declared as pseudoatoms with a pharmacophoric feature that is complementary to the respective anchor atom.

Two pseudoatom projection algorithms were implemented to find pseudoatoms opposing hydrogen bonding substructures of the reference ligand(s) (Table 1).

A linear geometry is found in, for example, hydroxy groups. In this case, a so called "linear" algorithm is used to find pseudoatoms within valid constraints (Figure 1 a). Based on the straight line from atom A to atom B, a region for validly positioned grid points is defined according to annotated distance and angle ranges (r_{min}, r_{max} and φ_{min}, φ_{max}).

Table 1. Overview of identified hydrogen bond geometries and their corresponding pseudoatom projecting algorithms ("linear" or "planar").

Geometry	Example	Geometry	Algorithm
		linear	linear
		planar with 3 atoms	planar
		planar with 4 atoms	planar
		tetrahedral	linear

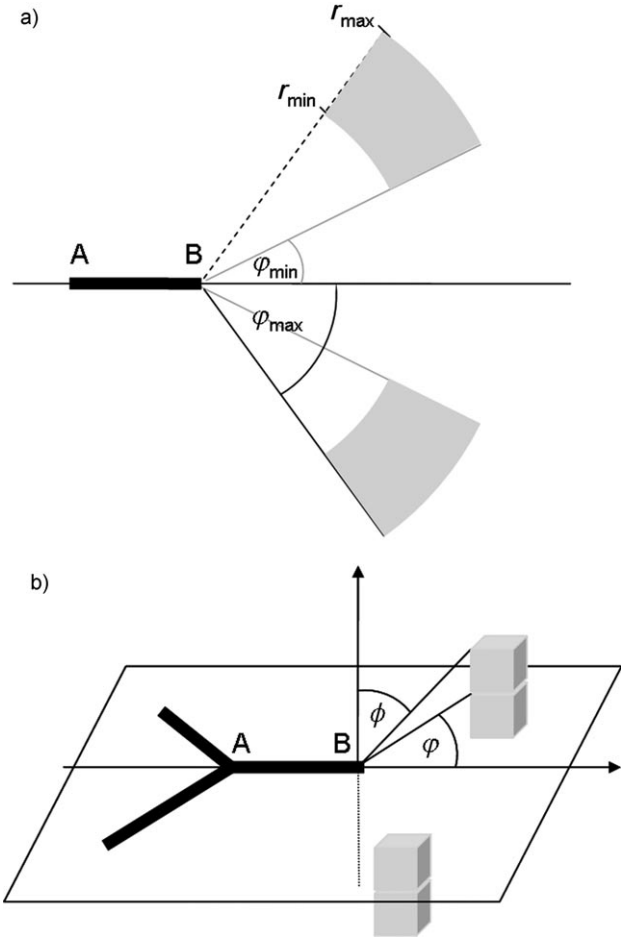

Figure 1. a) Schematic of the "linear" algorithm. Each grid point in the gray region around atom B has a valid interaction distance and angle. b) Schematic of the "planar" algorithm. Grid points in the shaded regions are declared as pseudoatoms.

Planar hydrogen bond geometries are found, for example, in carbonyl groups, where valid regions for pseudoatoms are positioned in the directions of the lone-pairs, which are in a plane with the sp2 hybridized carbon atom. An additional angle ϕ is required to define valid pseudoatom regions (Figure 1 b). When planar hydrogen bond geometries are based on only three ligand atoms, for example, an ether group, a virtual atom A is generated temporarily between the two connecting atoms.

The last case is observed in hydrogen bonds, where the interacting ligand atom has three neighboring atoms (tetrahedral geometry). Analogous to the first case, pseudoatom regions are identified by the "linear" algorithm after generation of a virtual atom centering the three neighbors to establish a straight line to the interacting ligand atom.

Substructures and pharmacophoric features

Ligand atoms that are capable of participating in hydrogen bonds were identified by a substructure search using molecular query language (MQL).[11] Table S1 in the Supporting Information denotes all ligand substructures, the employed projec-

tion algorithm, the pharmacophore type of the anchor atoms, and distance/angle constraints for defining valid pseudoatom regions around each anchor atom. As an extension to the hydrogen bond geometries, PRPS also employs aromatic pseudoatoms above and beneath benzene rings at a distance between 3.5 and 4.5 Å.[12]

Weighted pseudoreceptors

When pseudoreceptors are constructed around an aligned ligand ensemble, a pseudoatom weighting scheme is used, which computes a contribution weight w_{PA} for each pseudoatom. It reflects the relative importance of the pseudoatom expressed as the quotient of the number of molecules u, which generated the respective pseudoatom, and the total number of reference ligands v [Eq. (1)]. Pseudoatoms accessed by all reference ligands have a weight of 1.0, and pseudoatoms found by only one reference ligand have a weight of $1/v$.

$$w_{PA} = \frac{u}{v} \quad (1)$$

Correlation vector representation and screening

To use pseudoreceptors for rapid, alignment-free similarity searching, for example, in virtual screening applications, PRPS models were translated into a correlation vector representation.[13,14] A pseudoreceptor-derived correlation vector encodes the distance-based frequency of pseudoatom features present in the model. Three such pharmacophoric features (hydrogen bond acceptor, hydrogen bond donor, π stacking ["aromatic"]) were considered, resulting in six possible pseudoatom pairs (acceptor–acceptor, acceptor–donor, acceptor–aromatic, donor–donor, donor–aromatic, aromatic–aromatic). Pseudoatom pairs with a distance up to 15 Å (in 1 Å steps) were annotated in the correlation vector. This resulted in a 90-dimensional vector, giving the frequency *Freq* of pseudoatom pairs with features X and Y at distance d [Eq. (2)], where the Kronecker delta δ computes to 1, whenever a pair of the pseudoatoms i and j exists at distance d.

$$Freq_d(X,Y) = \sum_i^X \sum_j^Y \delta_d^{ij} \quad (2)$$

In the case of a pseudoreceptor model with weighted pseudoatoms, a weighted frequency was calculated by multiplication of pseudoatom weights w_i and w_j [Eq. (3)].

$$Freq_d(X,Y) = \sum_i^X \sum_j^Y \delta_d^{ij} w_i w_j \quad (3)$$

Virtual screening with pseudoreceptors was performed by ranking screening compounds according to their Euclidean distances to the pseudoreceptor correlation vector.

Molecular dynamics simulation of the H_4R

We calculated a H_4R homology model based on the β_2-adrenergic receptor template,[15] as its transmembrane domain sequence identity is higher (28%) than the second putative template (18%), the crystal structure of rhodopsin.[16]

The sequence alignment of the β_2-adrenergic receptor with H_4R is shown in Figure 2. The seven transmembrane helices of the 390-residue amino acid sequence of H_4R were aligned without gaps. The most conserved amino acids in the helices, such as the D(E)RY and the NpxxY sequence, and both cysteines, which form a disulfide-bridge, are aligned to their complementary amino acid. The amino acid sequence was truncated in the intracellular loop 3 between amino acid $214^{5.76}$ (5.76 according to the Ballesteros–Weinstein numbering system)[17] and $289^{6.21}$. Ten amino acids were deleted at the N terminus and 15 amino acids at the C terminus. The homology model was built using MODELLER 9v3.[18,19] The model was checked by PROCHECK[20] and WHATIF.[21] The Ramachandran plot (figure S1 in the Supporting Information) shows that 99.3% of the residues in the model are in favored regions. The average model score of the WHATIF Coarse Packing Quality Control test was −0.5, and only four amino acid residues have a WHATIF score below −5, all of which are found in intracellular loops.

This H_4R homology model was placed into a palmitoyl oleoyl phosphatidylcholine (POPC) lipid bilayer,[22] so that the eighth α helix was parallel to the membrane surface. Lipids

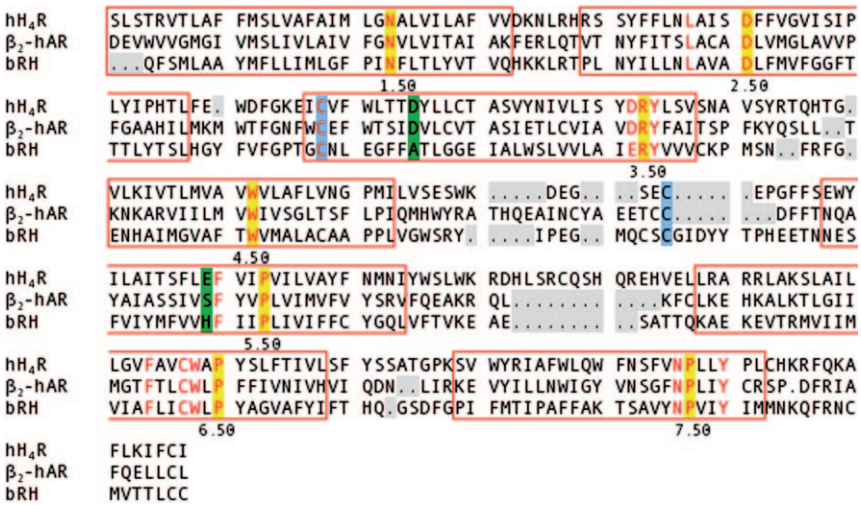

Figure 2. Sequence alignment of the human histamine H_4 receptor (hH_4R) and the β_2-adrenergic receptor (β_2-hAR). For comparison, the sequence of bovine rhodopsin (bRH) is shown as well. Transmembrane domains are indicated by red boxes. Conserved residues are in red letters. Position 50 in each transmembrane domain is marked in yellow, disulfide bridging residues are shown in blue, and residues $Glu182^{5.46}$ and $Asp94^{3.32}$ are in green.

were deleted within a distance of 0.8 Å from the protein and a TIP3P water model box was built around the protein–membrane complex.[23] This resulted in a system containing 10558 water molecules and 183 lipid molecules. Altogether, the simulation contained 60976 atoms.

The MD simulation was performed using NAMD2.6[24] with the CHARMM27 force field.[23,25] An integration step size of 2 fs was used; the vdW potential was smoothly decreased to zero between 8 and 12 Å. Electrostatic interactions were treated by the Particle mesh Ewald method.[26] The net charge was neutralized with six chlorine counterions. As an NPT ensemble was used, the number of atoms, pressure, and temperature were kept constant. The pressure was set to 1.01325 bar (1 atm), applying a modified Nosé–Hoover method,[27] and the system was coupled to a temperature bath at 310 K.

A cubic prism cell was used with an average phospholipid density of 0.78 ± 0.02 nm^2 and an average bilayer thickness of 3.31 ± 0.29 nm, which was assembled by the VMD Membrane Plugin 1.1 without additional equilibration. The thickness of the water slab was 2.5 nm at the top, and 2.0 nm at the bottom of the system.

The MD simulation was split into four phases: 1) energy minimization, 2) heating, 3) equilibration, and 4) production. The first phase was split into two minimization sections, were the Cα atoms were fixed during the first 2000 steps and harmonically restrained in the second minimization part (2000 steps). In the heating phase, the temperature was increased from 0 to 310 K over 12 ps. The motion of the Cα atoms in the heating and equilibration phase was still limited by harmonic constraints. After equilibration for 9 ps, the system was simulated without any constraints for 1 ns in the production phase.

Pseudoreceptor model of H_4R

We developed a pseudoreceptor model of the idealized H_4R ligand binding site based on five potent ligands compiled from published and patent information (Figure 3). Compounds **1**–**4** were aligned to an energy-minimized 3D conformation of JNJ7777120 using the software MOE v2007.09 (Chemical Computing Group, Montreal, QC (Canada) http://www.chemcomp.com). The constructed PRPS pseudoreceptor represents a putative consensus ligand binding mode (Figure 4).

From each frame of the H_4R MD simulation, pocket-forming amino acid coordinates were extracted as defined by Shin et al.[32] and Jongejan et al.[33] Binding pockets of each MD frame were prioritized according to their match with the pseudoreceptor. Only pseudoatoms with a weight $> 50\%$ were considered. In this way, we selected a potential binding pocket constellation that is capable of binding most of the reference ligands (Figure 5).

Figure 5a shows the resultant H_4R binding pocket, which suits best the pseudoreceptor. This perspective shows the pocket formed by the seven transmembrane domains viewed from the extracellular matrix. The H_4R pseudoreceptor's orientation is shown beside the pocket-forming amino acids. White spheres indicate those amino acid positions which fit the pseudoatom coordinates and pharmacophoric feature type precise-

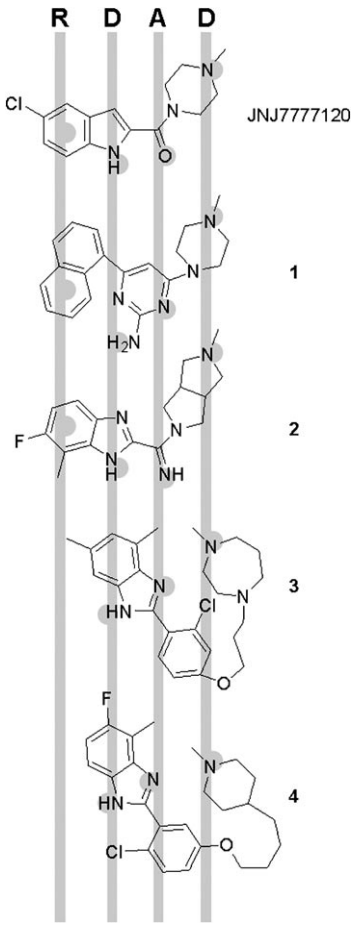

Figure 3. Reference ligands for H_4R pseudoreceptor generation: JNJ7777120 ($K_i = 4$ nM),[28] **1** ($K_i = 25$ nM),[29] **2** ($K_i = 4$ nM),[30] **3** ($K_i = 1$ nM), and **4** ($K_i = 1$ nM).[31] R: aromatic, D: hydrogen bond donor, A: hydrogen bond acceptor.

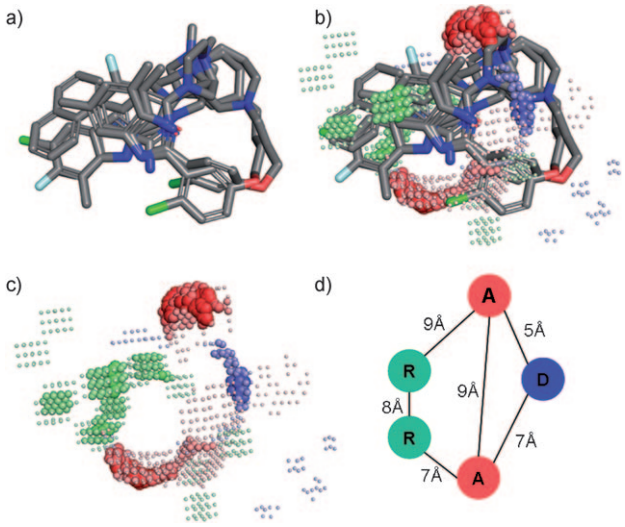

Figure 4. a) Ligand alignment and b) generated pseudoatoms, which form the c) H_4R pseudoreceptor. Panel d) presents a schematic of pseudoatom clusters projected by more than half of the reference ligands. Acceptor and donor pseudoatoms are shown in red and blue. Aromatic pseudoatoms are depicted as green spheres. The size of the spheres [in panels b) and c)] correlates with their relative importance [pseudoatom weight, w_{PA}; Eq. (1)].

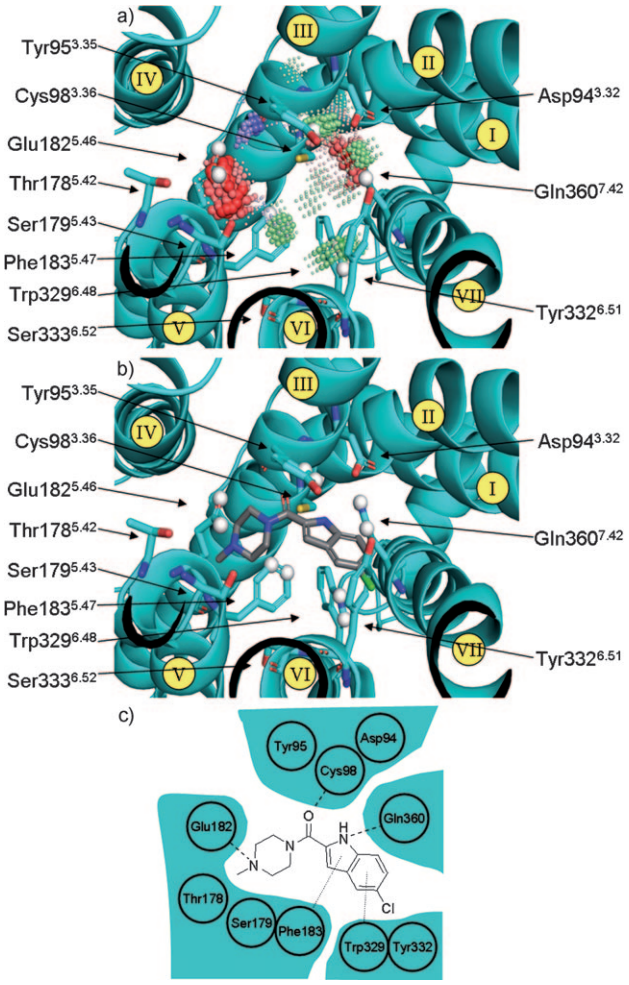

Figure 5. a) View from the extracellular matrix into the H_4R binding pocket showing the amino acid arrangement which fits best to the H_4R pseudoreceptor; Roman numerals in yellow circles indicate the transmembrane helix number. b) The potential orientation of the reference ligand JNJ7777120, and c) a 2D schematic of potential interactions; potential hydrogen bonds are drawn as dashed lines and aromatic interactions as dotted lines.

ly. Figure 5b shows the resultant orientation of the reference ligands. For the sake of clarity, only JNJ7777120 is depicted (see Figure 5c for a 2D schematic view), although all reference ligands are able to bind to the selected residue constellation. In the model arrangement, the basic moiety of the exemplarily shown reference ligand (methylpiperazine *N*-4 in JNJ7777120) seems to be able to interact with Glu182$^{5.46}$. Additional hydrogen bonds may exist from the amide oxygen to Cys98$^{3.36}$ and from the indole nitrogen to Gln360$^{7.42}$. Aromatic interactions to Trp329$^{6.48}$ and Phe183$^{5.47}$ might stabilize the conformation of helix VI, which has been postulated as a "receptor activity switch".[32]

During the MD simulations a preferred H_4R pocket amino acid constellation was found by PRPS. The suggested binding mode coincides with the hypotheses of Johart et al.[34] and Kiss et al.,[35] who postulated an interaction of the ligand's basic center to Glu182$^{5.46}$. Contrary to Jongejan et al.,[33] our adjusted model does not show free volume around Asp94$^{3.32}$. The observed complete loss of activity of JNJ7777120 in the Asp94Ala receptor mutant[33] can still be explained as a consequence of indirect effects resulting in a distortion of the ligand pocket geometry. In our MD simulations we also found pocket constellations supporting the conclusion of Jongejan et al., but we did not attempt to select a pocket for JNJ7777120 alone. Instead, we formulated a common binding hypothesis for several known antagonists and identified a plausible binding site, which is capable of interacting with all reference ligands. However, a definite binding mode should not be deduced from our model for JNJ7777120 or any other ligand.

PRPS revealed a promiscuous ligand binding pocket in H_4R by transferring multiple ligand information from a pseudoreceptor model, assuming a common binding mode for all reference ligands. It goes without saying that binding modes of agonists and antagonists might vary in H_4R, and the initial ligand alignment could be an artifact. Keeping this obvious caveat in mind, the adjusted receptor model is now ready for use by more sophisticated but more time-consuming receptor-based methods, for example, automated docking and in situ ligand de novo design.[1]

It is important to realize that automated docking of JNJ7777120 into the unrefined homology model and the pocket model selected by PRPS both resulted in plausible ligand–receptor complexes with favorable docking scores (figure S2, Supporting Information). This indicates that automated ligand docking into a GPCR homology model easily produces a seemingly meaningful result, which might correspond to an erroneous ligand pose. PRPS-based prioritization of a particular protein model obtained by MD simulation offers an opportunity for receptor model selection and might thus indirectly help improve virtual screening by automated ligand docking. We consider this application as the main potential benefit of PRPS.

Prospective screening for H_4R ligands

To probe the validity of the PRPS H_4R pseudoreceptor, we virtually screened a large compound library (562851 molecules). One heuristic 3D conformation was generated for each screening compound by CORINA v3.2 (Molecular Networks GmbH, Erlangen (Germany) http://www.molecular-networks.com). Acids were de-protonated and bases protonated using the software MOE v2007.09. This step is crucial as otherwise positive charges and implicit pharmacophoric features are not correctly identified in some substructures (for example, methylpiperazine). After encoding each screening compound into the appropriate molecular descriptor and ranking according to its Euclidean distance to the H_4R pseudoreceptor, we manually selected ten compounds from the first 0.05 percentile (281 molecules) of the ranked compound list. This selection was done to guarantee scaffold diversity among the selected candidates and avoid obvious hits (Figure 6).

Compounds were tested in a H_4R displacement assay[36] (Table 2), where **5** and **6** exhibited a $pK_i > 4$ ($K_i \sim 30$ μM). Notably, both compounds belong to different chemotypes, which demonstrates the potential applicability of the PRPS method to scaffold hopping.[37] The remaining molecules were considered inactive ($pK_i < 4$).

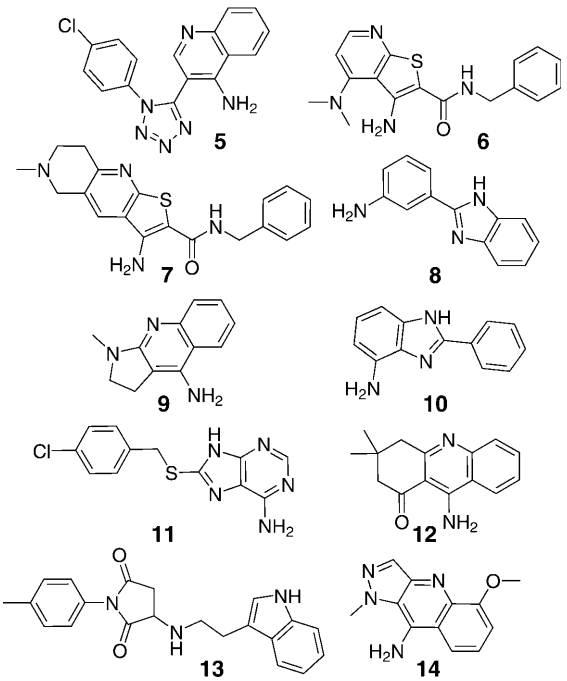

Figure 6. Compounds from pseudoreceptor-based virtual screening (one compound could not be delivered; details can be obtained from the compound providers; see Supporting Information table S2).

Table 2. Experimental H_4R affinity of ordered compounds.

Compd	Supplier collection	Affinity at hH_4R: pK_i[a]
5	Specs	4.5
6	Specs	4.5
7	Specs	<4
8	Asinex Gold	<4
9	Asinex Gold	<4
10	Asinex Gold	<4
11	Asinex Gold	<4
12	Asinex Gold	<4
13	Asinex Gold	<4

[a] Measurements were performed in at least two independent measurements; data are given as average values.

Conclusions

As a result of the availability of only a few reference protein structures, GPCR homology models are prone to modeling errors. MD simulations can be used to adapt and relax the initial models,[38] but fail to provide a single "best" ligand–receptor complex for virtual screening. Our deterministic pseudoreceptor concept PRPS transfers multiple ligand information into a receptor model to identify and prioritize a ligand binding pocket from a MD simulation of a H_4R homology model. This may establish new ways to select suitable target receptor models for use in receptor-based methods during drug design projects, where 3D target information is not available.

Docking of a known ligand into the receptor model taken from the initial and the selected frame of the MD simulation suggested potential binding poses. Notably, these poses differ strikingly for the initial and the selected protein model (figure S2, Supporting Information), which demonstrates that 1) although the PRPS algorithm does not yet explicitly consider hydrophobic interaction sites, it is applicable to finding potential ligand-binding pockets, and 2) PRPS complements automated docking approaches by prioritizing receptor models from a MD trajectory.

Retrieval of two new H_4R ligands by pseudoreceptor-based virtual screening demonstrated the general applicability of the PRPS descriptor in virtual screening (see Supporting Information for additional retrospective results, figure S3, table S3). The descriptor proved to encode biologically relevant pharmacophoric features in the PRPS model and provides an additional technique for finding new hits and leads in the early phases of drug discovery projects. Irrespective of such applications, we expect the main benefit from PRPS to be its combination with fast receptor-based virtual compound screening, as demonstrated herein for the H_4R model.

Experimental Section

Retrospective virtual screening

For retrospective validation of our software two pseudoreceptors were prepared. To avoid artifacts, which may occur during the ligand alignment procedure, we decided to use receptor-bound conformations determined by X-ray spectroscopy of multiple dihydrofolate reductase (DHFR) and factor Xa (fXa) inhibitors. In the case of DHFR, four complexes were selected to compute the pseudoreceptor model: 1DHF, 1DDR, 1DG5, and 1DG7.[39,40] The protein structures were superposed by minimizing the root mean square deviation between the Cα atoms using MOE v2007.09. The resulting alignment of DHFR inhibitors was used for calculation of the pseudoreceptor. The X-ray crystal structures of the fXa complexes 1EZQ, 1F0R, 1F0S,[41] 1FJS,[42] and 1KSN[43] were prepared in the same manner as the DHFR complexes. The COBRA 6.1 database containing 8311 known drugs and druglike molecules,[44] amongst which are 64 DHFR inhibitors and 228 fXa inhibitors, was screened with the cross-correlation descriptor derived from the pseudoreceptor models. Receiver–operator curves (ROC) are shown in figure S3 in the Supporting Information.[45] The curves indicate that the descriptor derived from the pseudoreceptor is suitable for enrichment of active compounds. Additional retrospective results are presented in table S3 (see Supporting Information), giving the proportion of retrieved actives per percentile of cyclooxygenase-2, factor Xa, angiotensin converting enzyme, PPARα/δ/γ, 5-lipoxygenase, dihydrofolate reductase, and thrombin ligands.

Compound libraries

For prospective virtual screening, the commercially available compound collections were pooled: Specs (v04/2008, 202681 compounds, Delft (the Netherlands) http://www.specs.net); Asinex-Gold (v11/2007, 233554 compounds); and Asinex-Platinum (v11/2007, 126616 compounds, Moscow (Russia) http://www.asinex.com).

Geometric hashing

Geometric hashing is an algorithm for the recognition of spatial similarity between two or more point sets.[46] It consists of three consecutive phases: 1) buildup, 2) search, and 3) evaluation.[47] During buildup, each triplet of pseudoatoms (with edges ranging from 5 to 15 Å) of the pseudoreceptor (query set) were enumerated. Each triplet is described by its three interpoint distances. Using distances instead of point coordinates leads to translation and rotation invariant description of the triplets. The distances were used in full precision as hash keys including information concerning the pharmacophoric features of each point to fill a hash table. In the second phase, a set of pocket-forming points (of a certain frame in the MD simulation) was used for a search in the hash table (candidate set). Distances and features were used in the same way as before to generate hash table keys. Each time a distance triplet was generated which already existed in the hash table, the respective key received a vote. Non-corresponding keys were dropped. Keys with votes represent corresponding subsets between the query and the candidate set. These triplets were extracted and aligned to each other by a transformation matrix, which was used to transform all remaining coordinates. After complete transformation a spatial proximity check was done. If points were closer than 1 Å to each other, they were tagged as matching points, as they support the overall match of the query and candidate set.

Binding assay

Prior to the experiments, cell membranes were sedimented by 10 min centrifugation at 4 °C and 13 000 rpm (Heraeus Biofuge Fresco; max. speed = 13 000 rpm, r_{max} = 8.5 cm: 16 000 *g*) and resuspended in binding buffer (12.5 mM $MgCl_2$, 1 mM EDTA, 75 mM Tris-HCl, pH 7.4). Competition binding experiments were carried out by incubating membranes, 35 μg well^{-1} (prepared from Sf9 cells expressing hH_4R, co-expressed with G-protein $G\alpha_{i2}$ and $G\beta_1\gamma_2$ subunits) in a final volume of 0.2 mL containing binding buffer and [^{3}H]histamine (10 nM, 566.1 GBq mmol^{-1}). Assays were run at least in duplicate with seven appropriate test compound concentrations between 1 nM and 100 μM. Incubations were performed for 60 min at 25 °C with shaking at 250 rpm. Nonspecific binding was determined in the presence of 100 μM unlabeled histamine. Bound radioligand was separated from free radioligand by filtration through GF/B filters pretreated with 0.3% (*m*/*v*) polyethyleneimine and washed with chilled (4 °C) binding buffer (3 × 0.5 mL). The amount of radioactivity collected on the filter was determined by liquid scintillation counting.

Acknowledgements

This research was supported by the Beilstein-Institut zur Förderung der Chemischen Wissenschaften, the LOEWE Lipid Signaling Forschungszentrum Frankfurt (LiFF), and the DAAD (D/06/25529).

Keywords: drug design · GPCR · homology models · molecular dynamics · virtual screening

[1] G. Schneider, K. H. Baringhaus, *Molecular Design—Concepts and Applications*, Wiley-VCH, Weinheim, **2008**.
[2] Y. Tanrikulu, G. Schneider, *Nat. Rev. Drug Discovery* **2008**, *7*, 667–677.
[3] G. Scapin, *Curr. Pharm. Des.* **2006**, *12*, 2087–2097.
[4] J. J. Lacapère, E. Pebay-Peyroula, J. M. Neumann, C. Etchebest, *Trends Biochem. Sci.* **2007**, *32*, 259–270.
[5] E. Granseth, S. Seppälä, M. Rapp, D. O. Daley, G. von Heijne, *Mol. Membr. Biol.* **2007**, *24*, 329–332.
[6] S. Costanzi, *J. Med. Chem.* **2008**, *51*, 2907–2914.
[7] M. A. Lill, *Drug Discovery Today* **2007**, *12*, 1013–1017.
[8] A. Tropsha, A. Golbraikh, *Curr. Pharm. Des.* **2007**, *13*, 3494–3504.
[9] Y. Kato, A. Itai, Y. Iitaka, *Tetrahedron* **1987**, *43*, 5229–5236.
[10] J. E. J. Mills, P. M. Dean, *J. Comput. Aided Mol. Des.* **1996**, *10*, 607–622.
[11] E. Proschak, J. K. Wegner, A. Schüller, G. Schneider, U. Fechner, *J. Chem. Inf. Model.* **2007**, *47*, 295–301.
[12] G. B. McGaughey, M. Gagné, A. R. Rappé, *J. Biol. Chem.* **1998**, *273*, 15458–15463.
[13] G. Moreau, P. Broto, *Noveau J. Chimie* **1980**, *4*, 757–759.
[14] S. Renner, G. Schneider, *J. Med. Chem.* **2004**, *47*, 4653–4664.
[15] S. G. Rasmussen, H. Choi, D. M. Rosenbaum, T. S. Kobilka, F. S. Thian, P. C. Edwards, M. Burghammer, V. R. Ratnala, R. Sanishvili, R. F. Fischetti, G. F. Schertler, W. I. Weis, B. K. Kobilka, *Nature* **2007**, *450*, 383–388.
[16] K. Palczewski, T. Kumasaka, T. Hori, C. A. Behnke, H. Motoshima, B. A. Fox, I. L. Trong, D. C. Teller, T. Okada, R. E. Stenkamp, M. Yamamoto, M. Miyano, *Science* **2000**, *289*, 739–745.
[17] J. A. Ballesteros, H. Weinstein, *Methods Neurosci.* **1995**, *25*, 366–428.
[18] A. Šali, T. L. Blundell, *J. Mol. Biol.* **1993**, *234*, 779–815.
[19] N. Eswar, M. A. Marti-Renom, B. Webb, M. S. Madhusudhan, D. Eramian, M. Shen, U. Pieper, A. Šali, *Curr. Protoc. Bioinf.* **2000**, *Suppl. 15*, 5.6.1–5.6.30.
[20] R. A. Laskowski, M. W. MacArthur, D. S. Moss, J. M. Thornton, *J. Appl. Crystallogr.* **1993**, *26*, 283–291.
[21] G. Vriend, C. Sander, *J. Appl. Crystallogr.* **1993**, *26*, 47–60.
[22] A. D. MacKerell, Jr., B. Brooks, C. L. Brooks III, L. Nilsson, B. Roux, Y. Won, M. Karplus in *The Encyclopedia of Computational Chemistry* (Ed.: P. v. R. Schleyer), Wiley, Chichester, **1998**, pp. 271–277.
[23] W. L. Jorgensen, J. Chandrasekhar, J. D. Madura, R. W. Impey, M. L. Klein, *J. Chem. Phys.* **1983**, *79*, 926–935.
[24] J. C. Phillips, R. Braun, W. Wang, J. Gumbart, E. Tajkhorshid, E. Villa, C. Chipot, R. D. Skeel, L. Kale, K. Schulten, *J. Comput. Chem.* **2005**, *26*, 1781–1802.
[25] B. R. Brooks, R. E. Bruccoleri, B. D. Olafson, B. J. States, S. Swaminathan, M. Karplus, *J. Comput. Chem.* **1983**, *4*, 187–217.
[26] T. Darden, D. York, L. Pedersen, *J. Chem. Phys.* **1993**, *98*, 10089.
[27] G. J. Martyna, D. J. Tobias, M. L. Klein, *J. Chem. Phys.* **1994**, *101*, 4177.
[28] J. A. Jablonowski, C. A. Grice, W. Chai, C. A. Dvorak, J. D. Venable, A. K. Kwok, K. S. Ly, J. Wei, S. M. Baker, P. J. Desai, W. Jiang, S. J. Wilson, R. L. Thurmond, L. Karlsson, J. P. Edwards, T. W. Lovenberg, N. I. Carruthers, *J. Med. Chem.* **2003**, *46*, 3957–3960.
[29] H. Sato, K. Fukushima, M. Shimazaki, K. Urbahns, K. Sakai, F. Ganter, K. Bacon, WO 2005/014556, **2005**.
[30] C. A. L. Lane, D. A. Price, WO 2006/056848A1, **2006**.
[31] K. L. Arienti, J. G. Breitenbucher, D. J. Buzard, J. P. Edwards, M. D. Hack, H. Khatuya, D. E. Kindrachuk, A. Lee, J. D. Venable, WO 2005/044807A2, **2005**.
[32] N. Shin, E. Coates, N. J. Murgolo, M. J. Morse, M. Bayne, C. D. Strader, F. J. Monsma, *Mol. Pharmacol.* **2002**, *62*, 38–47.
[33] A. Jongejan, H. D. Lim, R. A. Smits, I. J. P. de Esch, E. Haaksma, R. Leurs, *J. Chem. Inf. Model.* **2008**, *48*, 1455–1463.
[34] A. Johart, R. Kiss, B. Viskolcz, G. M. Keserű, *J. Chem. Inf. Model.* **2008**, *48*, 1199–1210.
[35] R. Kiss, B. Noszál, A. Rácz, A. Falus, D. Erős, G. M. Keserű, *Eur. J. Med. Chem.* **2008**, *43*, 1059–1070.
[36] E. H. Schneider, D. Schnell, D. Papa, R. Seifert, *Biochemistry* **2009**, *48*, 1424–1438.
[37] G. Schneider, W. Neidhart, T. Giller, G. Schmid, *Angew. Chem.* **1999**, *111*, 3068–3070; *Angew. Chem. Int. Ed.* **1999**, *38*, 2894–2896.
[38] S. A. Adcock, J. A. McCammon, *Chem. Rev.* **2006**, *106*, 1589–1615.
[39] J. F. Davies 2nd. , T. J. Delcamp, N. J. Prendergast, V. A. Ashford, J. H. Freisheim, J. Kraut, *Biochemistry* **1990**, *29*, 9467–9479.
[40] R. Li, R. Sirawaraporn, P. Chitnumsub, W. Sirawaraporn, J. Wooden, F. Athappilly, S. Turley, W. G. Hol, *J. Mol. Biol.* **2000**, *295*, 307–323.
[41] S. Maignan, J. P. Guilloteau, S. Pouzieux, Y. M. Choi-Sledeski, M. R. Becker, S. I. Klein, W. R. Ewing, H. W. Pauls, A. P. Spada, V. Mikol, *J. Med. Chem.* **2000**, *43*, 3226–3232.
[42] M. Adler, D. D. Davey, G. B. Phillips, S. H. Kim, J. Jancarik, G. Rumennik, D. R. Light, M. Whitlow, *Biochemistry* **2000**, *39*, 12534–12542.

[43] K. R. Guertin, C. J. Gardner, S. I. Klein, A. L. Zulli, M. Czekaj, Y. Gong, A. P. Spada, D. L. Cheney, S. Maignan, J. P. Guilloteau, K. D. Brown, D. J. Colussi, V. Chu, C. L. Heran, S. R. Morgan, R. G. Bentley, C. T. Dunwiddie, R. J. Leadley, H. W. Pauls, *Bioorg. Med. Chem. Lett.* **2002**, *12*, 1671–1674.
[44] P. Schneider, G. Schneider, *QSAR Comb. Sci.* **2003**, *22*, 713–718.
[45] A. Givehchi, G. Schneider, *Mol. Diversity* **2005**, *9*, 371–383.
[46] H. J. Wolfson, I. Rigoutsos, *IEEE Comput. Sci. Eng.* **1997**, *4*, 10–21.
[47] R. Norel, D. Fischer, H. J. Wolfson, R. Nussinov, *Protein Eng.* **1994**, *7*, 39–46.

Received: December 13, 2008
Revised: February 5, 2009
Published online on ■■ ■■, 2009

A new pseudoreceptor modeling method (PRPS) was applied to the refinement of a homology model of the human histamine H_4 receptor (H_4R), the prediction of a ligand binding site, and virtual screening. Retrieval of two new H_4R ligands demonstrates the biological relevance of the pseudoreceptor model and provides a means for finding new hits and leads in the early phases of drug discovery.

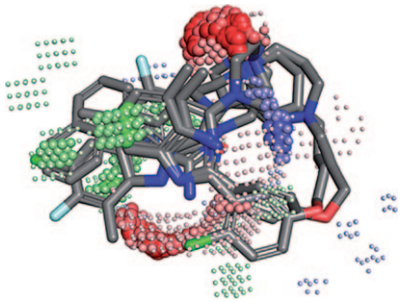

*Y. Tanrikulu, E. Proschak, T. Werner, T. Geppert, N. Todoroff, A. Klenner, T. Kottke, K. Sander, E. Schneider, R. Seifert, H. Stark, T. Clark, G. Schneider**

■■ – ■■

Homology Model Adjustment and Ligand Screening with a Pseudoreceptor of the Human Histamine H_4 Receptor

